ISBN: 978-3-95450-231-8 ISSN: 2673-5490 doi: 10.18429/JACoW-IPAC2023-TUPL142

BEAM DYNAMICS FOR THE RUEDI MICROSCOPY BEAMLINE *

J. K. Jones†, B. Hounsell, J. W. McKenzie, B. D. Muratori
ASTeC, STFC Daresbury Laboratory, Sci-Tech Daresbury, Warrington, UK
& also at the Cockcroft Institute, Sci-Tech Daresbury, Warrington, UK

Abstract

RUEDI is a proposed relativistic ultrafast electron diffraction and imaging facility for the UK. It will deliver single-shot time-resolved imaging with MeV electrons, as well as ultrafast electron diffraction at 10 fs timescales. The few-MeV-scale imaging/microscopy line aims to deliver high charge (up to 10^8 electrons), ultra-low emittance electron bunches to a 10 µm sample with minimal energy spread and transverse divergence, aiming for imaging resolutions at the 10 nm scale. The physical layout of the imaging beamline will be discussed, along with a multi-dimensional study of the beam dynamics of the proposed design. The extreme requirements on the injector specification, and the limitations inherent in such systems, have been investigated, and potential upgrade paths explored in terms of both imaging resolution and technological feasibility.

INTRODUCTION

The Relativistic Ultra-fast Electron Diffraction and Imaging (RUEDI) project, as encapsulated in the RUEDI Outline Instrument Design (OID) [1–3], consists of a low-emittance S-band photo-injector [4] operating at 4 MeV kinetic energy and injecting into either a time-resolved ultra-fast electron-diffraction beamline, or a high-energy transmission electron microscope (TEM) for ps-scale pump-probe experiments. The ultra-fast electron-diffraction beamline is described elsewhere [5].

The imaging beamline aims to operate in two modes: single-shot mode with 10^8 electrons per pulse (~20 pC), achieving ~10 nm resolution; and a stroboscopic mode with 10^6 electrons per pulse (~200 fC), achieving ~1 nm resolution per shot. The nominal beamline design is based around transverse focusing solenoidal magnets, maintaining cylindrical symmetry throughout. An alternative design based on the use of quadrupole magnets is also under consideration [6].

This paper will describe the initial design of the imaging beamline and the beam dynamics issues arising from inherent limitations.

BASELINE DESIGN

The RUEDI imaging line consists of four main components: (1) a 4 MeV S-band RF photo-injector; (2) transport and focusing of the electron beam to the sample using two solenoidal condenser lenses; (3) a sample chamber surrounded by a high-field solenoidal objective lens; (4) transport and magnification in the imaging line using two solenoidal projector lenses to focus the beam on to an imaging diagnostic. An RF cavity is included in the beamline to de-chirp and decelerate the electron bunch.

Objective Lens and Beam Energy

We can approximate the microscope resolution (r) , assuming spherical (C_s) and chromatic (C_c) aberration coefficients using Eq. 1.

$$r = \sqrt{\left(C_s \alpha^3\right)^2 + \left(C_c \alpha \delta\gamma/\gamma\right)^2} \tag{1}$$

with α, the objective aperture collection semi-angle, and $\delta\gamma/\gamma$, the relative beam energy spread. The achievable resolution of the microscope is proportional to the beam emittance and energy spread at the sample.

The aberration coefficients are dominated by the field quality of the objective lens. An initial study has shown that a reasonable upper limit for a compact normal-conducting solenoid lens is around 1.7 T, which gives aberration coefficients of around 10 mm. Using Eq. 1 we can achieve an ultimate resolution of ~1 nm assuming realistic emittance (~10 nm) and energy spread (~10^{-4}) values at a beam energy of 2 MeV.

At the nominal gun energy of 4 MeV the objective lens field must be higher to maintain the same focal length, which causes saturation of the magnet steel, reducing the field quality at the sample. As a result, the aberration coefficients become significantly worse and the achievable resolution is then far larger . The magnet will also need to be significantly larger and require much higher ampere-turns at this energy. The nominal beam energy for the solenoidal imaging line is therefore assumed to be 2 MeV.

Due to both space-charge forces on the cathode and operational considerations from a shared injector, it is advantageous to maintain the 4 MeV electron beam from the gun, which must then be decelerated before the 2 MeV objective lens. An RF cavity is placed very close to the sample chamber, to minimise space-charge-induced emittance dilution, combining both deceleration and de-chirping in the same cavity. To save space, the second condenser lens is wrapped around this cavity.

Layout

The layout of the RUEDI facility is shown in Fig. 1. The imaging line has a shared 4 MeV injector with the diffraction line, which utilises additional quadrupole magnets to match into the diffraction-line compression arc. These four quadrupoles are switched off for injection into the imaging line, and transverse focusing is provided only by the gun solenoid magnet. Two more solenoid magnets (condenser

* Work supported by EPSRC/UK Infrastructure Fund under grant number EP/W033852/1
† james.jones@stfc.ac.uk

ISBN: 978-3-95450-231-8 ISSN: 2673-5490 doi: 10.18429/JACoW-IPAC2023-TUPL142

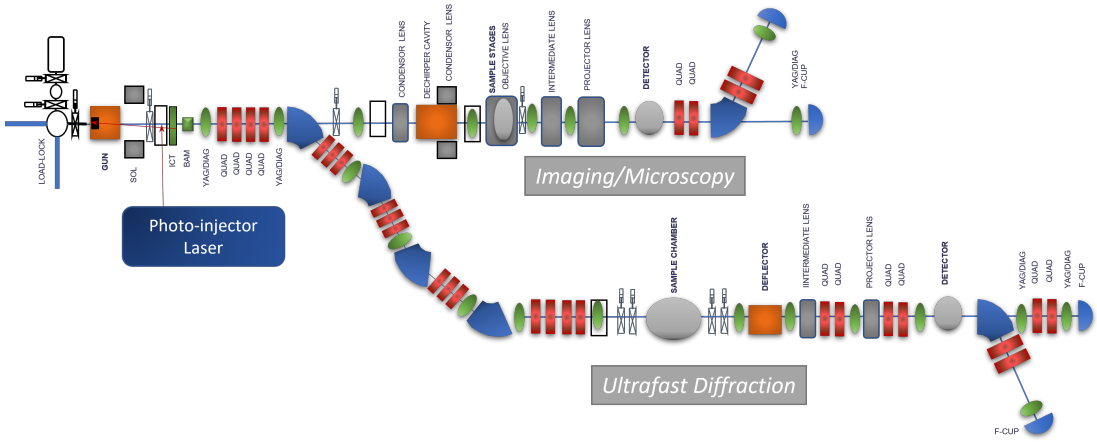

Figure 1: Proposed layout of the RUEDI facility showing the imaging and electron diffraction beamlines and the shared low-emittance injector.

lenses) are used to match into the sample located in the high-field solenoidal objective lens. The decelerating and de-chirping cavity is shown inside the second condenser lens. The objective lens is followed by two solenoidal lenses (intermediate and projector) that provide a beam magnification up to ~6500 at the detector - a direct electron, high resolution camera. This is followed by a spectrometer beamline for invasive energy measurements. Standard diagnostics, including beam position monitors and screen imaging stations, are distributed throughout the beamline, with locations to be finalised. Not shown in the schematic layout are the various secondary sources required for pump-probe experiments, including a wide array of laser-based and proton-beam sources. The possible suite of such sources is under active discussion with potential users.

Deceleration and De-chirping

The decelerating cavity should be a (sub-)harmonic of the gun frequency (2.9985 GHz), with the optimum frequency depending on the beam pulse length, since we wish to minimise the energy spread and must therefore minimise any additional RF curvature imprinted on the bunch during the deceleration process.

Due to space-charge forces at higher charges, the transverse emittance is inversely proportional to the electron pulse length, whilst the RF-curvature induced energy spread is proportional to the electron pulse length and the RF frequency. Thus, the optimum decelerating cavity frequency is inversely proportional to bunch charge and ideally at, or below, the gun frequency. In this study we assume a same-harmonic S-band cavity. The cavity must both decelerate and de-chirp the electron bunch, and this should occur as close to the sample as possible due to space-charge dilution of the emittance at 2 MeV. However, this implies a finite longitudinal chirp during transport from the electron gun through multiple solenoid lenses (gun and condenser), potentially significantly affecting the achievable emittance at the sample due to chromatic dilution of the emittance.

Additional studies will investigate the addition of a higher-order RF dechirping cavity at the exit of the gun combined with a same-order decelerating cavity at the sample to mitigate some of these issues. This harmonic cavity can also be used for additional chirp-control in the diffraction line.

RESULTS

Gun and Decelerating Cavity Only

We can estimate the optimum resolution limits using Eq. 1, and normalised emittance and energy-spread values calculated using GPT [7] for a simplified model of the machine, with only gun and dechirping cavity included. The results, excluding the solenoidal lenses and any post-sample transport, for 200 fC and 20 pC are shown in Fig. 2 and Fig. 3 respectively. Without the effects of chromatic aberrations from the solenoidal condenser lenses, the optimum working point is at +5° / 5 ps for the 200 fC case and +5° / 11 ps for the 20 pC case. This gives optimal resolution values of ~1 nm at 200 fC and ~125 nm at 20 pC, assuming a sample spot-size of 10 µm. Larger spot sizes reduce the calculated resolution, since the beam divergence (α in Eq. 1) at the focus decreases with increasing values of the β-function, but also reduces the electron density and thus can degrade the signal-to-noise ratio at the detector.

Gun to Sample Design

200fC Using the results in Fig. 2, an optimised solution at 200 fC, including solenoidal lenses, has been designed at a gun phase of +5° and laser pulse length of 5 ps, and is shown in Fig. 4. The solution uses a gun solenoid lens 0.42 m from the gun. This solenoid position must be tuned for both the imaging and diffraction lines, and is currently under active optimisation. One or two further condenser solenoids are used to match into the objective lens, which is positioned at 3.625 m from the cathode. The optimised solution uses one condenser lens for ease of optimisation, however only minor resolution improvements were found using two condenser

ISBN: 978-3-95450-231-8 ISSN: 2673-5490 doi: 10.18429/JACoW-IPAC2023-TUPL142

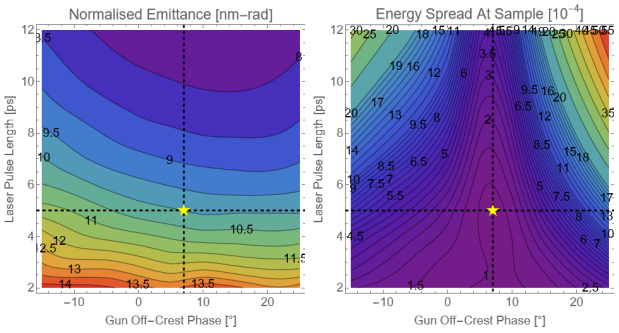

Figure 2: Normalised emittance and energy spread at the exit of the dechirping cavity as a function of gun phase and laser pulse length for 200fC bunch charge from the gun. The nominal working point is highlighted.

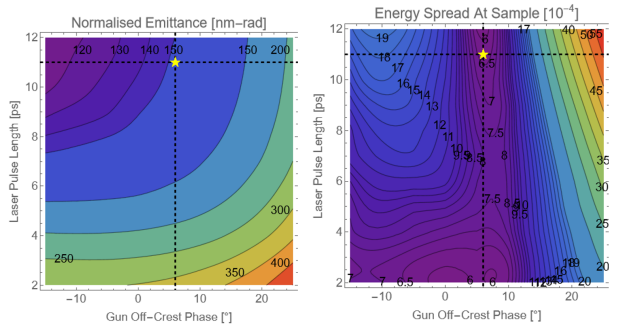

Figure 3: Normalised emittance and energy spread at the exit of the dechirping cavity as a function of gun phase and laser pulse length for 20pC bunch charge from the gun. The nominal working point is highlighted.

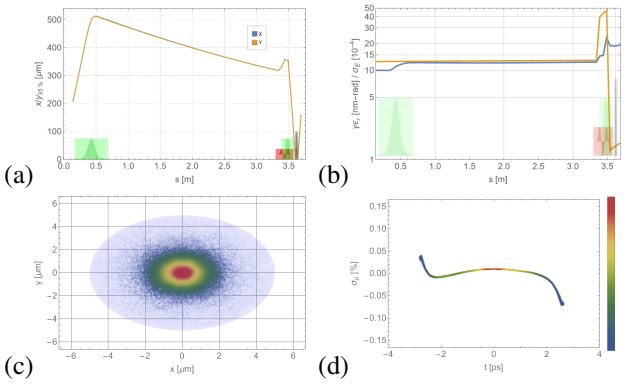

Figure 4: (a) Transverse beam sizes, (b) transverse emittances, (c) transverse phase space, and (d) longitudinal phase space at the sample for the 200 fC working point.

lenses since the chromatic emittance increase is relatively small in these lenses. The final estimated resolution for this mode, *not including the projector section*, is <1 nm.

20pC The same methodology has been used for the 20 pC design, with a gun phase of +5° and laser pulse length of 11 ps, and shown in Fig. 5. Only one solenoidal condenser lens is used. The results show a spot size of 30 µm, rather than the design value of 10 µm and this corresponds with a

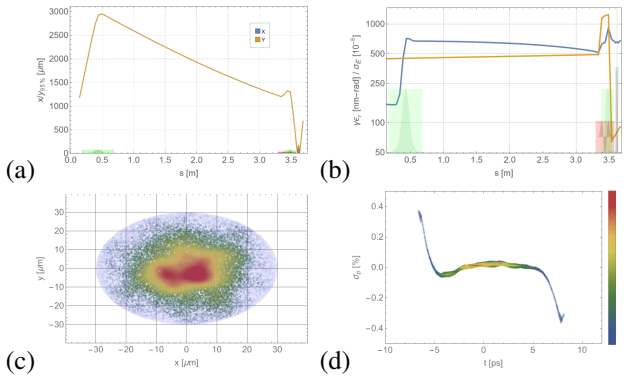

Figure 5: (a) Transverse beam sizes, (b) transverse emittances, (c) transverse phase space, and (d) longitudinal phase space at the sample for the 20 pC working point.

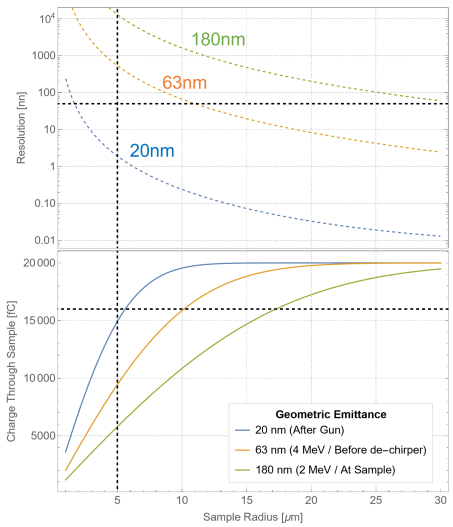

Figure 6: Scaling of the resolution (top) and charge transmission (bottom) of the electron beam at 20 pC for different sample radii.

normalised emittance value of 45 nm−rad and a β-function value of ~1 mm at 2 MeV. Achieving spot sizes smaller than this at 20 pC bunch charge is challenging. In Fig. 6 we show the calculated resolution and charge transmission as a function of sample radii at specific locations in the beamline, demonstrating the significant effect of the chromatic emittance increase due to the solenoidal focusing lenses and the relative increase in geometric emittance from decelerating the electron bunch to 2 MeV.

CONCLUSION

Initial studies have been performed of the RUEDI imaging line injector performance. Imaging resolutions of ~1 nm are shown to be possible from the injector at 200 fC bunch charges and 2 MeV after deceleration from a gun energy of 4 MeV. At 20 pC we cannot achieve the required spot size on the sample of 10 µm, but that with a larger spot size of 30 µm we can achieve injector resolutions of ~40 nm.

ISBN: 978-3-95450-231-8 ISSN: 2673-5490 doi: 10.18429/JACoW-IPAC2023-TUPL142

REFERENCES

[1] T. C. Q. Noakes *et al*, "RUEDI Outline Instrument Design", 2022.

[2] J. W. McKenzie *et al.*, "Establishing a Relativistic Ultrafast Electron Diffraction & Imaging (RUEDI) UK National Facility", presented at the IPAC'23, Venice, Italy, May 2023, paper TUPL144, this conference.

[3] RUEDI, http://www.ruedi.uk/.

[4] B. Militsyn *et al.*, "Conceptual design of the low dark charge photocathode RF gun for Relativistic Ultrafast Electron Diffraction and Imaging (RUEDI) facility", presented at IPAC'23, Venice, Italy, May 2023, paper TUPA029, this conference.

[5] B. Hounsell *et al.*, "Beam dynamics of the RUEDI diffraction beamline", presented at IPAC'23, Venice, Italy, May 2023, paper TUPL145, this conference.

[6] B. D. Muratori *et al.*, "RUEDI Microscopy: Solenoids or Quadrupoles?", presented at IPAC'23, Venice, Italy, May 2023, paper WEPL062, this conference.

[7] "Pulsar Physics, General particle tracer", http://www.pulsar.nl/gpt